Effect of different nanoparticles on the properties and enzymatic hydrolysis mechanism of aliphatic polyesters

4 AUTHORS:

Dimitrios N Bikiaris
Aristotle University of Thessaloniki
297 PUBLICATIONS **6,970** CITATIONS

SEE PROFILE

Nikos Nianias
École Polytechnique Fédérale de Lausanne
7 PUBLICATIONS **60** CITATIONS

SEE PROFILE

Evrykleia Karagiannidou
Pharmathen
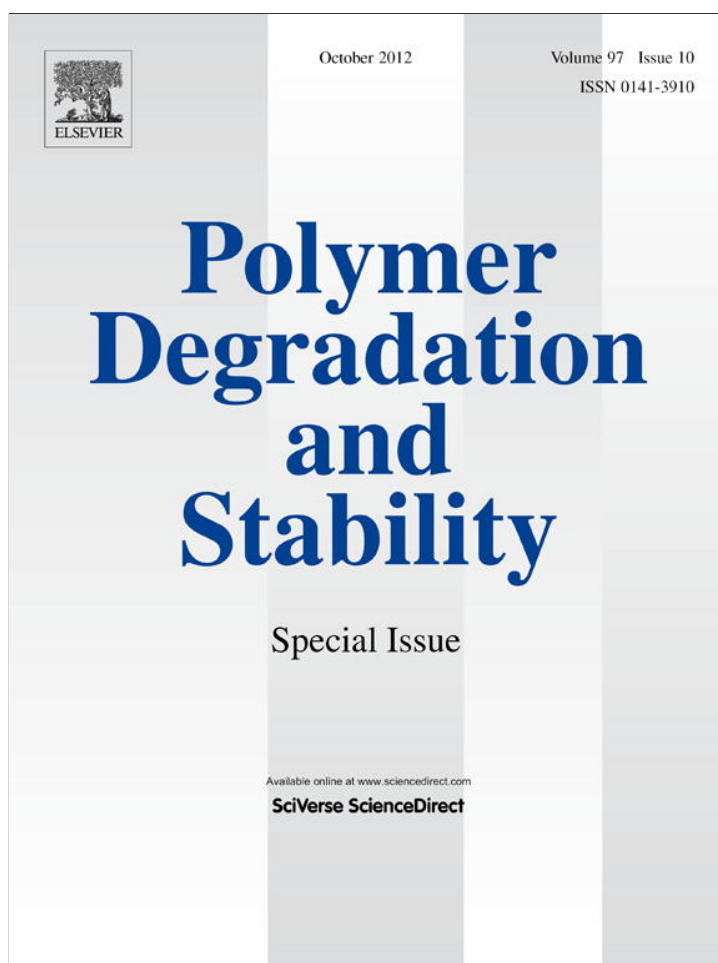**20** PUBLICATIONS **47** CITATIONS

SEE PROFILE

Aristides Docoslis
Queen's University
55 PUBLICATIONS **978** CITATIONS

SEE PROFILE

Effect of different nanoparticles on the properties and enzymatic hydrolysis mechanism of aliphatic polyesters

Dimitrios N. Bikiaris [a,*], Nikolaos P. Nianias [a], Evrykleia G. Karagiannidou [b], Aristides Docoslis [c]

[a] Laboratory of Polymer Chemistry and Technology, Department of Chemistry, Aristotle University of Thessaloniki, GR-541 24 Thessaloniki, Macedonia, Greece
[b] Pharmathen Industrial S.A., 9th klm Thessaloniki-Thermi, 57001 Thessaloniki, Greece
[c] Department of Chemical Engineering, Queen's University, Kingston, ON K7L 3N6, Canada

ABSTRACT

In the present study poly(propylene sebacate) (PPSeb) nanocomposites containing 2 wt% of either fumed silica nanoparticles (SiO_2), multiwalled carbon nanotubes (MWCNTs), or montmorillonite (MMT) were prepared by in situ polymerization. TEM micrographs confirmed that the dispersion of the nanoparticles was homogeneous in the PPSeb matrix, although some small agglomerates were observed, mainly in SiO_2 nanocomposites. The tensile strength and Young's moduli were significantly increased in nanocomposites due to the addition of nanoparticles. The reinforcement effect of nanoparticles was also established through Dynamic Themomechanical analysis (DMA). Mass loss measurements showed that, when compared to neat PPSeb, the presence of nanoparticles results in reduced enzymatic hydrolysis rates. This is due to the hindering effect of nanoparticles on the action of the enzymes since the former reduce the available surface area for hydrolysis, but also due to the interactions taking place between nanoparticles and PPSeb matrix. The mechanism of enzymatic hydrolysis was investigated by molecular weight variation and LC-MS analysis of the soluble by-products. It was found that PPSeb and its nanocomposites have identical hydrolysis mechanisms; even thought nanocomposites have lower hydrolysis rates.

1. Introduction

Biodegradable polymers are attracting a high level of interest. Among them, aliphatic polyesters like poly(L-lactic acid), poly(e-caprolactone) (PCL), poly(butylene succinate) (PBSu), poly(3-hydroxybutyrate), poly(3-hydroxyvalerate) and others represent a very important class due to their desired features of biodegradability and biocompatibility. Such polymers are now being considered for use in both biomedical and consumer applications. Until recently, polyesters derived from ethylene glycol and 1,4-butanediol dominated because of difficulties in the preparation of 1,3-propanediol (1,3-PD) in sufficient quantities and purity. In recent years, more attractive processes have been developed for the production of 1,3-PD from renewable resources, and research on related polymers has attracted interest from both industrial and academic perspectives. Polyesters of 1,3-PD exhibit good properties and high biodegradability [1]. PPSeb is a biodegradable aliphatic polyester prepared from 1,3-PD and 1,10-decanedioic acid (an aliphatic diacid) [2]. Sebacic acid (SA) is an intermediate product of ω-oxidization of long-chain aliphatic acid. Compared with short-chain aliphatic acids, SA is more suitable for the preparation of polyesters, as short-chain aliphatic acids always conduce to intra-molecular condensation. However, published work on polyesters of sebacic acid is scarce. PPSeb has tensile strength that is slightly lower than that of low density polyethylene [2], a fact that may reduce its applications. In order to increase the mechanical properties, nanoparticles can be added to the PPSeb matrix. Polyester nanocomposites draw an ever-increasing attention due to the tremendous enhancement that can impart on the mechanical, thermal, optical, and structural properties of the pristine material [3]. Compared to conventional composites, polymer nanocomposites maximize the polymer–nanoparticle interactions since the filler is dispersed on a nanometer scale, thus creating an extremely high interfacial area per unit volume of compositae.

The enzymatic degradation of biodegradable polyesters is sensitive to their chemical structure, hydrophilic/hydrophobic balance within the main chain, molecular weight and crystallinity. Now it is generally accepted that crystallinity acts as a hindrance to biodegradability. Biodegradation first takes place in the amorphous region where the erosion rate is much higher than in the crystalline region. A survey of the literature reveals that there is great confusion regarding the biodegradation of aliphatic polyester nanocomposites.

In most cases an increase of the biodegradation rate was observed with the addition of nanoparticles [4–12]. It was concluded that the more hydrophilic the filler, the more pronounced the degradation [4]. This behaviour was also explained by the presence of Al Lewis acid sites in the inorganic clays which catalyze the ester linkages hydrolysis. Similar results were reported for PLA or PCL and clay nanocomposites, which after 5 months in *Bacillus licheniformis* liquid culture showed only 10% of residual mass, as opposed to 60% observed in pure PLA [5]. Obviously, the biodegradability of several aliphatic polyesters is significantly enhanced after nanocomposite preparation with clays [6,7]. As reported by Ray et al. [8] the presence of terminal hydroxylated edge groups of the silicate layers is one of the responsible factors for the degradation. The hydrolysis of aliphatic polyesters in nanocomposites completely depends upon both the nature of pristine layered silicates and surfactants used for the modification of layered silicate [9].

Enhanced biodegradation rates were also reported when using other nanoparticles with aliphatic polyesters. According to Han et al. the relative rate of biodegradation observed in PBSu/silica nanocomposites was faster than that of neat PBSu, indicating dependence on silica content [10]. The proposed explanation, as in the case of layered silicates, was that the increased hydrophilicity of the material due to the presence of hydroxyl groups on the fumed silica's surface enhanced its susceptibility to microbial attack. Chouzouri et al. found that the incorporation of calcium silicate or Bioglass 45S5 appeared to enhance the degradation behaviour of both PCL and PLA [11]. Enhanced degradation behaviour was attributed to the fact that the hydrophilic fillers enhanced the degree of swelling of the otherwise hydrophobic matrix [12].

However, completely different findings regarding the effect of nanoparticles on the biodegradation behaviour have also been reported. Lee and co-workers [7] observed that the biodegradation rate of nanocomposites of aliphatic polyesters was decreased by the presence of layered silicates. They attributed this to the difficulty for the micro-organisms to reach the bulk matrix due to the barrier properties of the clay nanoparticles that make the diffusion path more tortuous. Recently, Maiti et al. [13] also reported that the biodegradability of the poly(hydroxybutyrate)/OMLS nano-composite system was reduced after the addition of organically modified layered silicates. Such reductions of the biodegradation rate have been related to interactions of the matrix with the nano-filler, but also to water permeability, degree of crystallinity and anti-microbial property of the nano-fillers studied. In a recent work the degradation of aliphatic polyesters like PLA, PCL and their nanocomposites based on an unmodified sepiolite were studied in compost [14]. It was found that despite the significant degradation levels achieved for both materials, the presence of sepiolite particles seemed to partially delay the PLA matrix degradation. Similar results were also reported by Fukushima et al., in PCL/nanoclays, the addition of the latter partially delayed the rate of polymer degradation in compost, probably due to a more difficult pathway for micro-organisms in order to attack the PCL ester groups [15].

In the present work, the synthesis and comparative study of three nanocomposites of PPSeb containing either MWCNTs, SiO₂, or MMT prepared by in situ polymerization are presented. Emphasis was given to the study of the effect of nanoparticles on the enzymatic hydrolysis of PPSeb, as well as to the comparison between our findings and those reported in the literature concerning the aliphatic polyesters.

2. Experimental

2.1. Materials

Sebacic acid (SA) (purum 99%), tetrabutyl titanate [Ti(OBu)₄] of analytical grade and poly(phosphoric acid) (PPA) used as heat stabilizer were purchased from Aldrich. 1,3-Propanediol (1,3-PD) (CAS number 504-63-2, purity >99.7%) was supplied by Du Pont de Nemours. Cloisite 20A (MMT) were supplied by Southern Clay Products (Gonzales, TX) and is a montmorillonite modified with dimethyl(dihydrogenated tallow)ammonium salts, whose organic content is 29.2 wt%, as determined by TGA. The MWCNTs used in this work were synthesized by the chemical vapour deposition (CVD) process and were supplied by Nanothinx (Patra, Greece). Fumed silica nanoparticles (SiO₂) used for nanocomposites preparation, were supplied by Degussa AG (Hanau, Germany) under the trade name AEROSIL® 200, having a specific surface area 200 m²/g, SiO₂ content >99.8% and average primary particle size 12 nm.

2.2. Polyester and in situ synthesis of nanocomposites

PPSeb was prepared by the two-stage melt polycondensation method (esterification and polycondensation) in a glass batch reactor. In brief, proper amounts of SA and 1,3-PD (molar ratio 1:1.2) and Ti(OBu)₄ catalyst were charged into a 250 cm³ round-bottom flask of the polycondensation apparatus. The apparatus with the reagents was evacuated several times and filled with argon in order to remove all oxygen. Thereupon, the mixture was heated under a nitrogen atmosphere for 3 h at 190 °C under constant stirring (350 rpm) and water was removed by distillation as the reaction by-product of esterification. In the second step of polycondensation, PPA was added (5×10^{-4} mol PPA/mol Sebacic acid), and vacuum (5.0 Pa) was applied slowly over a period of time of about 30 min, to avoid excessive foaming and to minimize oligomer sublimation. The temperature was slowly increased to 230 °C, while stirring speed was also increased to 720 rpm. The polycondensation continued for about 60 min for all prepared polyesters.

For the in situ synthesis of nanocomposites the same procedure was used but prior to the addition of SA the proper amount of each nanoparticle was added and dispersed by ultrasonic vibration (50W, Hielscher UP50H) for 20 min in 1,3-PD. The right mass of SA was then added and the aforementioned polycondensation method was followed for the in situ synthesis of nanocomposites. Three different nanocomposites were prepared containing 2 wt% SiO₂, 2 wt% MWCNTs and 2 wt% MMT.

2.3. Nanocomposites characterization

2.3.1. Gel permeation chromatography (GPC)

GPC analysis was performed using a Waters 150C GPC system with differential refractometer as detector and three ultrastyragel (103, 104, 105 Å) columns in series. CHCl₃ was used as the eluent (1 ml/min) and the measurements were performed at 35 °C. Calibration was performed using polystyrene standards with a narrow molecular weight distribution.

2.3.2. Mechanical properties

Measurements of the tensile mechanical properties of the prepared nanocomposites were performed on an Instron 3344 dynamometer, in accordance with ASTM D638, using a crosshead speed of 5 mm/min. Relative thin sheets of about 350 ± 25 μm were prepared using an Otto Weber, Type PW 30 hydraulic press connected with an Omron E5AX Temperature Controller, at a temperature of 90 ± 5 °C. The moulds were rapidly cooled by immersing them in water at 20 °C. From these sheets, dumb-bell-shaped tensile test specimens (central portions 5 × 0.5 mm thick, 22 mm gauge length) were cut in a Wallace cutting press and conditioned at 25 °C and 55−60% relative humidity for 48 h. From stress-strain curves the values of Young's modulus, elongation at break and tensile strength at the break point were determined. At least five

specimens were tested for each sample and the average values, together with their standard deviations, are reported.

2.3.3. Scanning electron microscopy (SEM)

The morphology of the prepared samples in the form of films before and after enzymatic hydrolysis was examined in a SEM system (JEOL JMS-840). The films were covered with a carbon coating in order to provide good conductivity of the electron beam. Operating conditions were: accelerating voltage 20 kV, probe current 45 nA, and counting time 60 s.

2.3.4. Transmission electron microscopy

Electron diffraction (ED) and transmission electron microscopy (TEM) observations were made on ultra thin film samples of the various nanocomposites prepared by an ultra-microtome. These thin films were deposited on copper grids. ED patterns and TEM micrographs were obtained using a JEOL 120 CX microscope operating at 120 kV. To avoid the destruction of the films after exposure to the electron irradiation, an adequate sample preparation is required, thus, the thin films were coated with carbon black.

2.3.5. Differential scanning calorimetry (DSC)

The thermal behaviour of the nanocomposites was studied using a Perkin−Elmer Pyris Diamond DSC differential scanning calorimeter. The instrument was calibrated with high purity indium and zinc standards. Samples of 6.0 ± 0.2 mg were used for every measurement. A constant nitrogen flow was maintained to provide a constant thermal blanket within the DSC cell, thus eliminating thermal gradients and ensuring the validity of the applied calibration standard from sample to sample. For each sample a cyclic scanning procedure was followed to record the thermal behaviour of the material. The procedure involved: (a) heating up to 80 °C at a heating rate of 20.0 °C min^{-1} and holding at this temperature for 3 min in order to erase any thermal history of the sample, (b) rapid cooling to −60 °C and equilibration for 2 min, c) reheating at a heating rate of 20 °C min^{-1} up to 80 °C.

2.3.6. Dynamic mechanical analysis (DMA)

The dynamic mechanical properties of the nanocomposites were measured with a Perkin−Elmer Diamond DMA. The bending (dual cantilever) method was used with a frequency of 1 Hz, a strain level of 0.04%, in the temperature range of −80.0 to 30.0 °C. The heating rate was 3 °C min^{-1}. Testing was performed using rectangular bars measuring approximately $30 \times 10 \times 3.0$ mm^3. These were prepared with a hydraulic press, at a temperature of 90 °C under a load of 50 kN on a ram of 110 mm, for a time period of 5 min, followed by quenching in ice water (~ 0 °C). The exact dimensions of each sample were measured before the scan.

2.3.7. Contact angle measurements

Contact angle measurements were carried out by the sessile drop method using a Krüss DSA 100 (Krüss) apparatus and distilled water as described previously [16]. Water droplets (2−4 μL) were delivered to different points of each specimen and from a height sufficiently close to the substrate so that the needle remained in contact with the liquid droplet. Then, the delivery needle was withdrawn with minimal perturbation to the drop, and the image of the drop was captured immediately for static (θs) contact angle measurement. The reported contact angle values are averages of five measurements.

2.3.8. X-ray photoelectron spectroscopy (XPS)

The element composition and interfacial interactions were studied using an X-ray photoelectron spectra (XPS). In the XPS analysis (AXIS Ultra 'DLD' X-ray photoelectron spectrometer),

a monochromatic Al Ka X-ray was used at 14 kV. A binding energy of 284.8 eV for the C 1s of aliphatic carbons was taken as the reference energy. The XPS curve fitting of C 1s, O 1s, Si 2p and Al 2p were accomplished using Kratos' Vision 2 Processing software.

2.4. Enzymatic hydrolysis

PPSeb and its nanocomposites in the form of films ($10 \times 20 \times 0.4$ mm^3, ~ 100 mg) were prepared using an Otto Weber Type PW 30 hydraulic press as described earlier. The films were placed in test tubes, wherein 5 ml of phosphate buffer solution (0.2 M, pH 7.2) was added, containing 0.09 mg/mL *Rhizopus delemar* lipase and 0.01 mg/mL *Pseudomonas cepacia* lipase. The loosely capped test tubes were kept at 37.0 ± 1.0 °C in an oven for 1 month while the media were replaced every 24 h. After a predetermined time the films were removed from the lipase solution, washed thoroughly with distilled water and ethanol and then dried at room temperature under vacuum, till constant weight. Every measurement was repeated three times. As a control, the same experiment was carried out under the same conditions without the addition of lipase. The degree of enzymatic hydrolysis was estimated from mass loss. All samples were studied with DSC, to estimate the changes in the degree of crystallinity, while the morphology of the films during enzymatic hydrolysis was examined using SEM (JEOL JMS-840) as described earlier. Furthermore, the liquid media comprising the buffer and hydrolysed fragments after every replacement (24 h) was studied with Liquid chromatography-mass spectrometry (LC-MS) in order to investigate the mechanism of enzymatic hydrolysis.

2.5. Liquid chromatography-mass spectrometry (LC-MS)

The LC-MS analysis of liquid media during enzymatic hydrolysis was performed using a Shimadzu quadrupole LC-MS with two Prominence LC pumps (LC-20AD), a degasser (DGU-20A3), a diode array detector (SPD-M20A), an autosampler (SIL-20AC) and a column oven (CTO-20AC). A 4.6*100 mm C$_{18}$, 5 μm analytical column (Symmetry Shield, Waters, USA) was used for the chromatographic separation. Both the autosampler and the column oven temperatures were set at 25 °C. The mobile phase had a flow rate of 0.8 ml/min and consisted of methanol and water in the proportion of 90:10v/v respectively. All samples were eluted isocratically.

The Shimadzu mass selective detector operated in Atmospheric Pressure Ionization mode and performed scanning monitoring, in positive and negative polarity, with scan speed at 4000 amu/sec. The following mass parameters were used: detector voltage at 1.7 kV, drying gas at 0.02 MPa, Interface temperature at 400 °C, CDL temperature at 250 °C, Heat Block temperature at 200 °C and nebulizing gas flow at 2.5 L/min.

3. Results and discussion

3.1. Nanocomposites synthesis and characterization

The PPSeb and PPSeb/nanocomposites were synthesized following direct polyesterification of 1,3-PD and sebacic acid. At the first stage of esterification oligomers are formed, which have average molecular weights between 1500 and 2000 g/mol, while water is removed as by-product [1]. In order to prepare a material having high molecular weight, the polycondensation of these oligomers took place at higher temperatures with the simultaneous application of high vacuum (Fig. 1). The number average molecular weight of PPSeb that was prepared according to the described procedure was 35260 g/mol (Table 1). In the case of nanocomposites
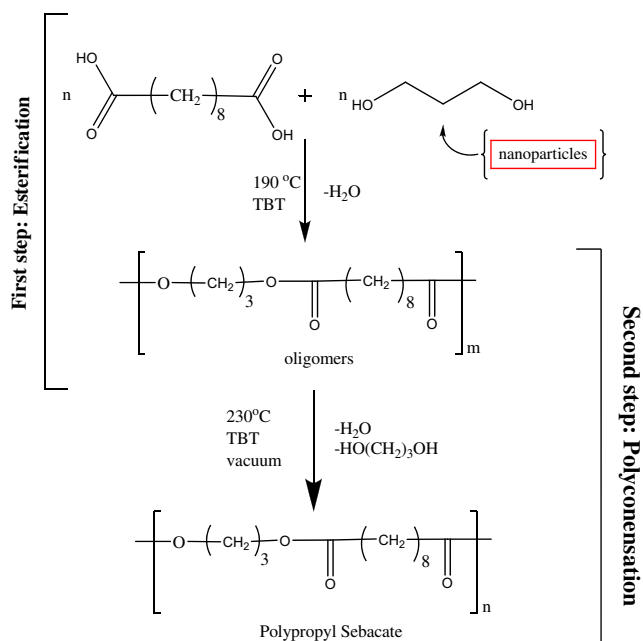
Fig. 1. Synthetic route via the two-step melt polycondensation of PPSeb and its nanocomposites.

one of the major problems is the fine dispersion of nanoparticles into polymer matrix. In most of the reported studies in the literature, the nanocomposites were prepared using solvent mixing or melt mixing methods, since these are very easy and economical methods. However, the main drawback of these methods is the poor dispersion of the nanoparticles into the polymer matrix. For this reason the in situ method was used in the present study. In order to avoid nanoparticle agglomeration, the overnight dried nanoparticles (MWCNTs, SiO_2 and MMT) were dispersed in the 1,3-PD prior to polycondensation and subjected to ultrasonic vibration for 20 min. This method was chosen since 1,3-PD, one of the monomers used for the preparation of PPSeb, is liquid. The addition of nanoparticles affected the esterification and mainly the polycondensation reaction [17,18] during synthesis of PPSeb and, thus, polyesters with higher molecular weights were prepared compared to neat PPSeb. This was in agreement with our previous studies [17–19].

In the case of PPSeb/SiO_2 nanocomposites the surface silanol groups ($\equiv$Si-OH) of fumed silica nanoparticles have a slightly acidic nature. This renders them capable of reacting with alcohols, just like an acid. The possibility of such a reaction between the surface silanol groups of fumed silica nanoparticles and the hydroxyl end groups of the polymer were first hinted in one of our previous studies on nanocomposites of poly(ethylene terephthalate) with fumed silica nanoparticles [20] Additional evidence was subsequently obtained from measurements performed by other authors using solid-state ^{29}Si-NMR and FTIR on nanocomposites of fumed silica with PET [21,22] and poly(butylene succinate) (PBSu) [10,17].

Furthermore, the formation of these bonds in a similar polyester like poly(propylene succinate) was also proved in our previous study by using XPS analysis [18]. These studies indicated the possibility of covalent bonding between the fumed silica nanoparticles and the PPSeb polymer backbone chain in our study and will be discussed in details in following part of this study. This reaction can also explain why PPSeb/SiO_2 nanocomposites have higher molecular weight than neat PPSeb. However, this cannot be explained in the case of PPSeb/MWCNTs nanocomposites since these nanoparticles, unlike SiO_2, have no such reactive groups; thus it is not possible for these nanoparticles to react with PPSeb macromolecules towards the formation of covalent bonds. In PPSeb/MMT nanocomposites MMT has some silica hydroxyl group, which could react with PPSEb. However, these are mainly due to structure defects and are located at the edges of MMT plates. Furthermore, due to their low magnitude they are not enough to participate in such reactions as SiO_2 and formation of covalent bonds during in situ polymerization of PPSEb.

To investigate the degree of dispersion of nanocomposites in the PPSeb matrix TEM was employed. From the collected micrographs it was found that the nanoparticles are homogeneously dispersed into the PPSeb matrix (Fig. 2). Individual nanoparticles appear in the samples, co-existing with some small agglomerates, as in the case of fumed silica nanoparticles. Because of the method that is used to prepare this type of nanoparticles (fumed silica) some individual spherical nanoparticles are chemically linked by SiOSi bridges [23]. For this reason it is not possible to obtain a dispersion of SiO_2 nanoparticles completely free of agglomerates since the latter were initially present in the raw material used for the composite's preparation. The shear stresses occurring during the in situ polymerization of PPSeb are not enough to break these agglomerates and disperse SiO_2 in the form of individual nanoparticles. A finer dispersion was achieved when MWCNTs and MMT nanoparticles were added in polyester matrix. Furthermore, the montmorillonite plates were completely separated, meaning that with the help of the organic modifier the polymer macromolecules were able to penetrate between the montmorillonite layers increasing the distance between them, ultimately leading to their separation. Therefore, the montmorillonite was dispersed in exfoliated form into the PPSeb matrix, thereby proving the effectiveness of the current procedure for the preparation of nanocomposites.

The thermal behaviour of PPSeb and PPSeb/nanocomposites was investigated with DSC and the results are presented in Table 1. Neat PPSeb has a melting point of 55.3 °C, heat of fusion 58.9 J/g and glass transition temperature of −52.5 °C. The glass transition values were found to be similar for the nanocomposites with PPSeb, while their heat of fusions and melting points were much higher. This is due to the nucleating effect of nanoparticles which cause a heterogeneous nucleation increasing the degree of crystallinity of PPSeb.

A differentiation can be also found in mechanical properties of nanocomposites. The tensile properties of all samples are presented in Table 1. As can be seen PPSeb is a brittle material, likely due to its low molecular weight, and its specimen breaks before the yielding

Table 1
Molecular weights, thermal and mechanical properties of PPSeb and its nanocomposites.

Samples	IV[a] (dL/g)	Mn (g/mol)	T_g (°C)	T_m (°C)	ΔH_m (J/g)	Tensile strength at break (MPa)	Elongation at break (%)	Young's modulus (MPa)
PPSeb	0.56	35260	−52.5	55.3	58.9	8 ± 1.1	8 ± 1	51 ± 3
PPSeb/SiO_2	0.72	52680	−52.9	62.1	64.8	11 ± 1.7	9 ± 1	303 ± 14
PPSeb/MMT	0.66	50790	−52.9	60.3	64.6	11 ± 1.7	13 ± 1.5	332 ± 14
PPSeb/MWCNTs	0.64	46570	−52.3	59.4	65.7	10 ± 1.3	6 ± 1	287 ± 13

[a] Intrinsic viscosity (IV) measurements were performed using an Ubbelohde viscometer cap. Oc at 25 °C in chloroform at a solution concentration of 1 wt%.
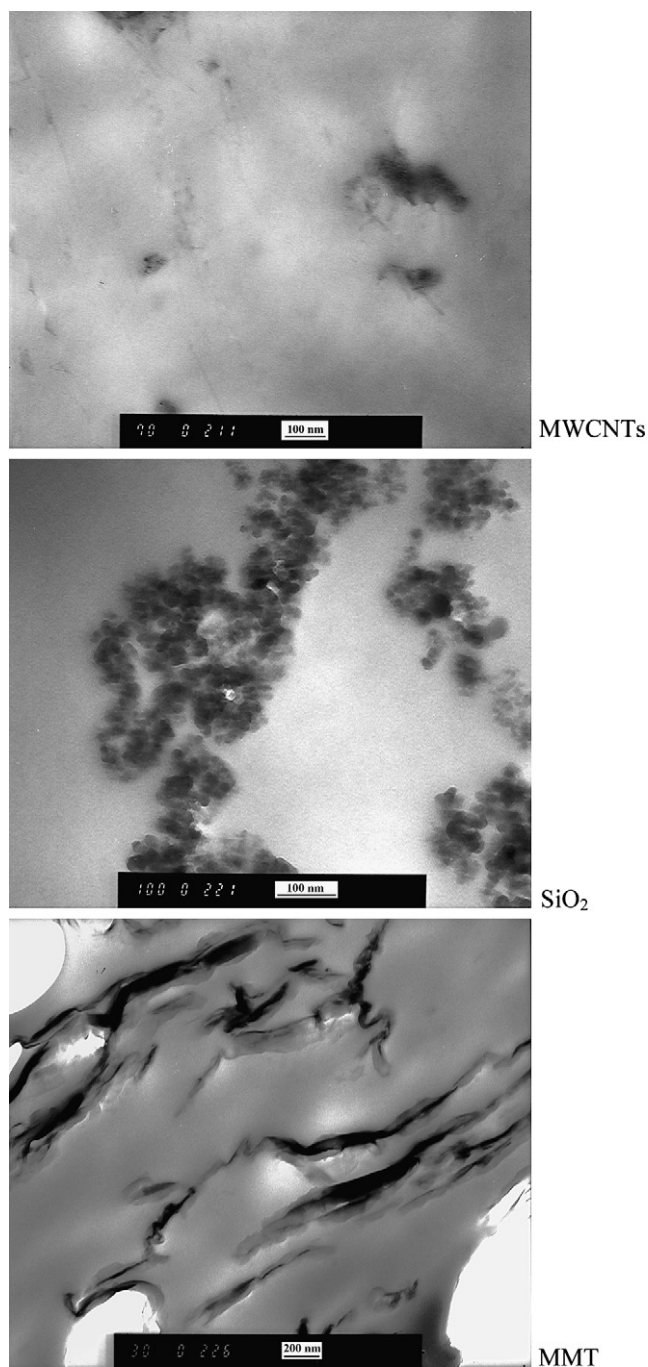
nanocomposites and higher than 300 MPa in nanocomposites containing SiO_2 and MMT. This could be the result of the presence of rigid nanoparticles finely dispersed in the polymer matrix, as well as interactions between nanoparticles and macromolecular chains, as in the case of SiO_2 nanoparticles. Silanol groups of SiO_2 can interact with hydroxyl end groups of PPSeb macromolecules forming covalent bonds. In all nanocomposites the nanoparticles act as reinforcing materials.

DMA was also used to study the prepared nanocomposites and the reinforcement effect of nanoparticles. The temperature dependence of the storage modulus (E') and tanδ for all prepared samples is presented in Fig. 3. E' gradually decreases with increasing temperature and a transition is observed between −60 and −10 °C, which is ascribed to the glass transition temperature of the material (T_g) [24]. At low temperatures the storage modulus is higher compared with neat PPSeb confirming the reinforcement effect of nanoparticles. The increase can be attributed to the restriction of the molecular motion of the PPSeb macromolecules due to the fine dispersion of the nano-fillers, which leads to increased interactions with the polymer matrix [17,25,26]. Another contributing factor is the reaction between the two phases, as in the case of SiO_2 nanocomposites, towards the formation of a covalent bond which further constrains the molecular motion of the macromolecular chains. The extent of this reinforcement is limited above the T_g due to the higher molecular motion of the PPSeb macromolecular chains. Thus above the T_g the storage modulus decreases sharply and all nanocomposites have almost similar storage moduli. The restricted molecular motion of nano-composites can also be seen from tanδ curve (Fig. 3b). In all nanocomposites this peak has smaller intensity, compared with neat PPSeb.

Fig. 2. TEM micrographs of PPSeb and its nanocomposites.
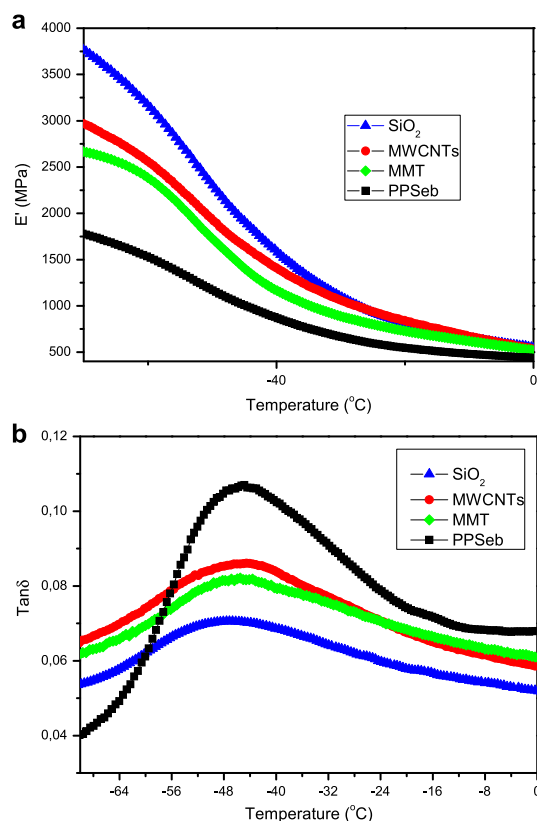
Fig. 3. Variation of a) storage modulus and b) tanδ as a function of temperature for the PPSeb nanocomposites recorded in DMA tests at a heating rate 3 °C/min and modulation frequency 1 Hz.

point. The addition of nano-filler cannot alter the mechanical behaviour of these nanocomposites as evidenced by the almost identical stress-strain curves recorded. However, the additions of nanoparticles have a positive effect on the tensile strength values (Table 1). From these results it can be noticed that tensile strength at break increased in all nanocomposites by about 30–40%. This increase is an indication of high adhesion between the polymer matrix and the inorganic nanoparticles. Furthermore, the lack of extended agglomerates, which could act as points of stress concentration that promote material failure, probably contributed to this behaviour. Finally, the addition of the nanoparticles induced a substantial increase in the Young's modulus, which increased from 51 MPa in neat PPSeb to 287 MPa in the PPSeb/MWCNTs

3.2. Enzymatic hydrolysis of nanocomposites

Polyesters having a relatively large number of methylene groups and those having α- and β-ester bonds as PPSeb with low T_m are hydrolysable by lipases [27]. As was reported in the experimental section, enzymatic hydrolysis of PPSeb and its nanocomposites was studied in aqueous solutions containing mixture of *R. delemar* and *Pseudomonas Cepacia* lipases, at 37 °C and pH = 7.2. Enzymatic hydrolysis rates of the nanocomposites were found significantly different from those of neat PPSeb. Fig. 4 shows the weight loss of the specimens, expressed as a fraction of 100 (percentage) of the initial mass of the specimen as a function of time of enzymatic hydrolysis. As can be seen, PPSeb showed the fastest enzymatic degradation among the tested samples, while PPSeb/nanocomposites showed a slower rate. Neat PPSeb was completely dissolved under 10 days of enzymatic treatment. The fumed silica nanoparticles slowed down enzymatic hydrolysis. This is in accordance with a previous study from Fukushima et al. who reported that the presence of fumed silica particles has a negative effect on the degradation level of PLA since it reduces macromolecular chain mobility [28]. However, these results are completely different to the findings in the case of PBSu/SiO$_2$ nanocomposites, where the nanocomposites reported that have higher hydrolysis rates that of neat PBSu [10]. Reduced hydrolysis rate was also found in PPSeb/MMT nanocomposite, which is in agreement with some reported findings in literature [7,13–15,29]. Clay-containing nanocomposites underwent a more difficult degradation, and they argued that this may possibly be due to the recalcitrant nature of clay towards biodegradation. Also Lee et al. [30] attributed the hindering effect of clay towards biodegradation to the fact that the barrier effect due to the filler prevents water from exerting hydrolysis. All these are in agreement with our study since the addition of MMT reduces the rate of enzymatic hydrolysis, compared with neat PPSeb. However, these are completely different to previous findings that reported enhanced biodegradation rates of aliphatic polyesters in the presence of layered silicates [4–9]. PPSeb/MMT nanocomposite has higher enzymatic hydrolysis rate form PPSeb/SiO$_2$ nanocomposite but lower than that of PPSeb/MWCNTs. In the case of PPSeb/MWCNTs nanocomposite, which exhibits the highest mass loss among the studied nanocomposites, there are no data reported by others on aliphatic polyesters and MWCNTs to which we could compare our findings (Fig. 5).
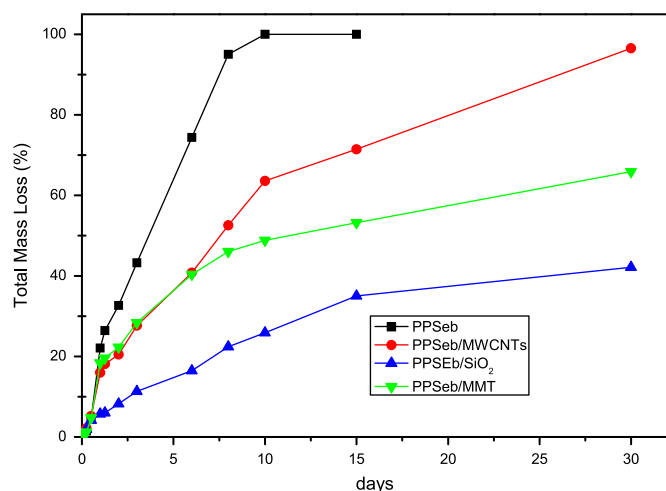
Enzymatic degradation of polyesters can be affected by several factors, having to do with the chemical structure, the type and amount of filler, the solid-state of the degraded specimen. Hydrophilic/hydrophobic balance segments within the main chain, molecular weight, frequency of ester bonds along the macromolecular chains, segmental mobility of the macromolecules as well as the degree of crystallinity, crystalline morphology, spherulite size and lamellar structure can also influence the rate of biodegradation [31,32]. Furthermore, enzymatic hydrolysis rates are anticipated to be faster at temperatures close to the melting point. Marten et al. found that hydrolysis shows significant rates only when the difference between the melting point and the temperature of hydrolysis is less than 30 °C [33,34]. Finally the glass transition temperature could affect the hydrolysis rates [35]. In our samples even though PPSeb has similar glass transition temperature with nanocomposites, its heat of fusion as well as its melting point is much lower. Both of these could have a small effect in enzymatic hydrolysis rate and can explain the lower rates of nanocomposites. The molecular weight could be also a notable factor for such differences since nanocomposites have higher molecular weights than neat PPSeb and this could justify the slower enzymatic hydrolysis rates observed. However, in this case nanocomposites should have similar rates with one another, since they have almost similar molecular weights, melting points and heat of fusions. From Fig. 4 it can be seen that this is not the case. From all these it can be inferred that the main factor that affects the hydrolysis rate is the kind of the filler used and, more specifically, the kind of interactions between the filler and macromolecular chains. Other factors such as, melting point, degree of crystallinity and molecular weight may have minor effects.

Weight loss measurements provide a general trend of the enzymatic hydrolysis, but don't reveal how this hydrolysis proceeds. Thus, the morphology of the prepared samples before and after enzymatic hydrolysis was examined using SEM micrographs. In spite of the fact that enzymatic hydrolysis is a heterogeneous process, as can be seen in Fig. 6 the whole surface of the samples had been eroded evenly on the first day of enzymatic hydrolysis. In the case of neat PPSeb enzymatic hydrolysis takes place mainly in amorphous areas, revealing intact areas with crystallites. This is seen clearly on the 8th day of hydrolysis. The appearance of the nanocomposites' surface is completely different from that of neat PPSeb. As it can be seen small fragments are removed from the surfaces but crystallites are not detected, as in neat PPSeb, even after 8th day of hydrolysis. This is because nanoparticles, acting as nucleating agents, are causing heterogeneous nucleation [36]. The addition of nanoparticles results in the increase of the number of spherulites and thus in a decrease of their diameter [37]. Thus surface deterioration is not as extensive as in the case of PPSeb. Even though the enzymatic hydrolysis rate was different between nanocomposites (Fig. 4), it was not possible to deduce such a differentiation from the recorded micrographs. This is because in all nanocomposites the size of spherulites is very small and almost identical.

From the above study using SEM it was found that the spherulite size can influence the enzymatic hydrolysis of nanocomposites since nanocomposites have smaller sizes compared with PPSeb. Taken into account that amorphous areas are first hydrolyzed, it seems that in nanocomposites the available surface area for hydrolysis is reduced, due to their higher degree of crystallinity and the existence of nanoparticles. According to Ozkoc et al., the hydrophilicity and crystallinity of PLA films are the main factors that can affect the biodegradation rates of nanocomposites [38]. This behaviour was attributed to the higher degree of crystallinity that the nanocomposites have compared with neat PLA, since nanoparticles accelerate the crystallization of PLA. Furthermore,

Fig. 4. Weight loss vs time plots for PPSeb nanocomposites during enzymatic hydrolysis.
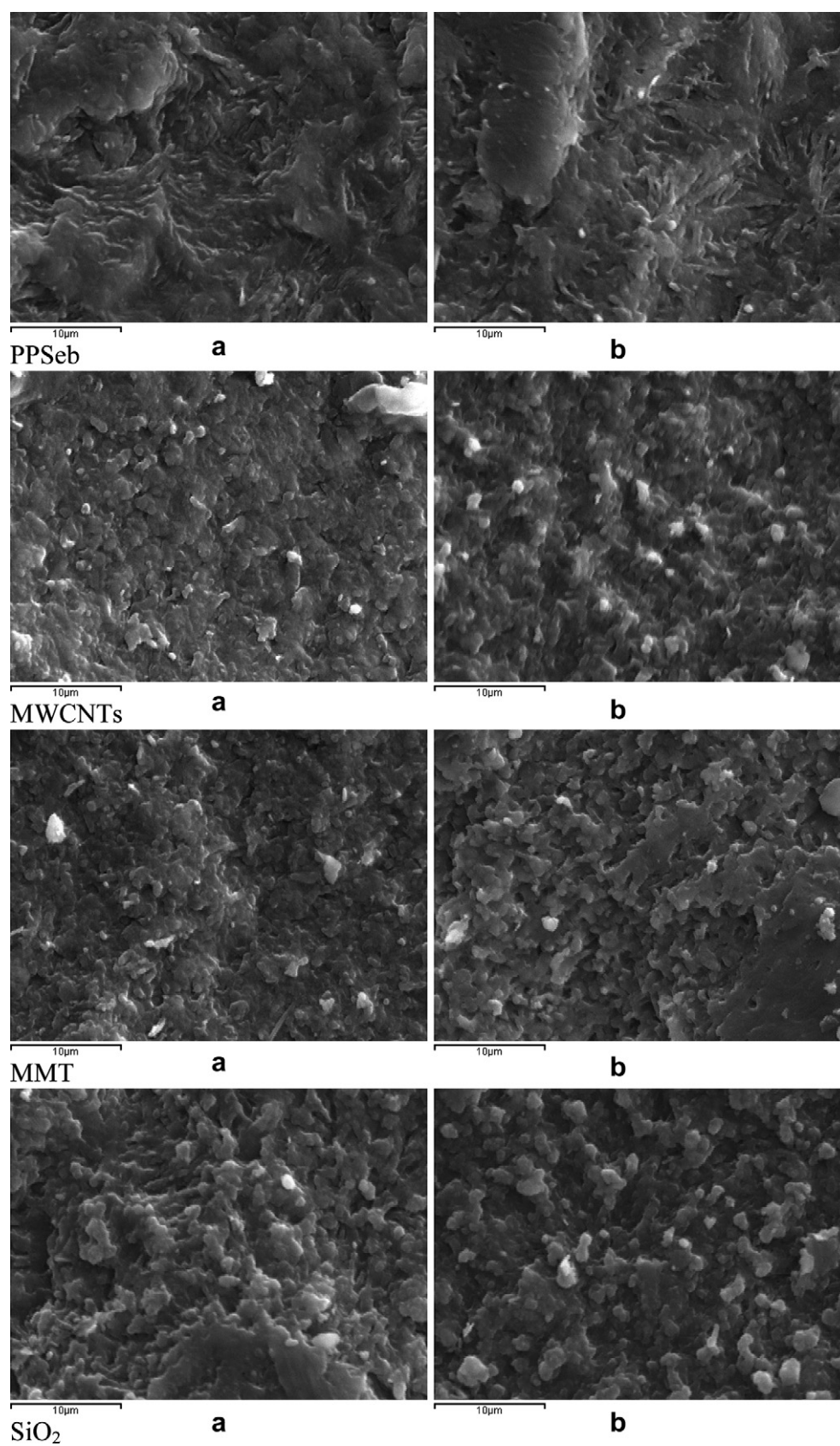
Fig. 5. SEM micrographs of PPSeb and its nanocomposites during enzymatic hydrolysis at different times a) 1 day and b) 8 days.
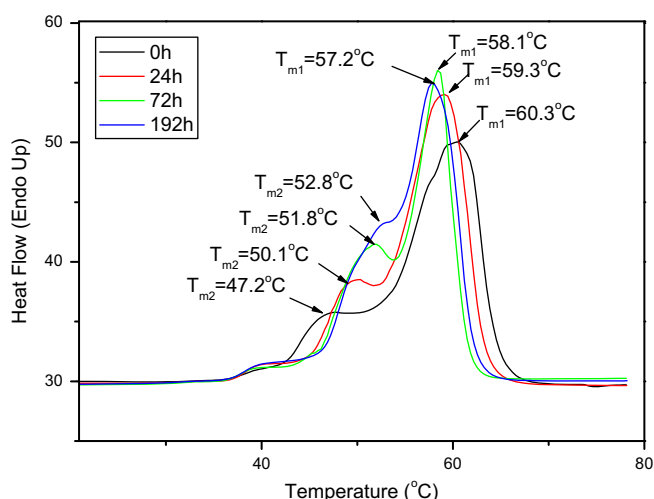
Fig. 6. DSC thermograms (fusion peaks) of PPSeb/MMT nanocomposites after enzymatic hydrolysis at different times (0 h, 24 h, 72 h and 192 h).

crystallization can be changed during enzymatic hydrolysis, since nanoparticles can act as nucleating agents, and this can also affect the rate of hydrolysis [9]. To understand the effect of crystalline structure on enzymatic hydrolysis and its alteration over time, the degree of crystallinity was monitored in all samples during enzymatic hydrolysis. Fig. 6 is an example of a DSC thermogram, corresponding to the case of the PPSeb/MMT, which captures the changes in the physical state of the sample as it undergoes enzymatic hydrolysis. It should be noted that similar behaviour was observed in all of the nanocomposites studied. Detailed results are reported in Table 2.

As can be seen all the samples have two melting peaks. In the initial sample the main and most characteristic peak is recorded at 60.3 °C (T_{m1}) and a smaller peak is recorded at 47.2 °C (T_{m2}). During enzymatic hydrolysis the first peak progressively shifts to lower values. The second peak shows the opposite trend and shifts to higher values while its magnitude increases. This behaviour could be attributed to the annealing that takes place during enzymatic hydrolysis, since at 37 °C the rearrangement of the macromolecular chains and formation of new crystals is possible. Furthermore, one additional factor could be the reduction of the amorphous part, since as was verified from SEM micrographs, the amorphous areas are more susceptible to enzymatic hydrolysis. Both of them result in an increase of the degree of crystallinity of the samples during enzymatic hydrolysis. This was also verified from the calculation of the heat of fusion of the samples and their degree of crystallinity (Table 2). The degree of crystallinity was calculated by taking the heat of fusion for completely crystalline material to be 140 J/g [39]. As can be seen from Table 2, the heat of fusion increases steadily in all samples until 72 h of enzymatic hydrolysis and after that time a plateau is reached. Furthermore, it is characteristic that all

nanocomposites have higher degree of crystallinity than neat PPSeb, which could be one reason for the lower hydrolysis rates that these nanocomposites exhibit. Similar increase in heat of fusion with biodegradation time was reported for the case of PCL/clay nanocomposites, whereas there was only a slight increase for neat PCL after 6 weeks of biodegradation [9]. However, the differences in the degree of crystallinity between nanocomposites are very small to explain the big differences observed in the mass losses of the samples.

It is known that the enzymatic degradation of polyesters occurs through the hydrolysis of ester bonds. Therefore, the degradation rate is associated with the ability of water to wet and subsequently absorb into the nanocomposites. In view of that, the hydrophilic or hydrophobic character of the nanoparticle can have a strong influence on the extent to which hydrolysis occurs. The hydrophobicity of the samples was evaluated by measuring their contact angle and water uptake. As can be seen from Fig. 7 PPSeb has a contact angle of 92.5°, which is similar to that of PPSeb/SiO$_2$ nanocomposites (91.8°). From the other nanocomposites PPSeb/MMT seems to be the most hydrophilic since due to the high hydrophilic nature of the clay it has the lowest contact angle ca. 80.6° while PPSeb/MWCNTs has the highest contact angle from all samples ca. 112.8°. From the water uptake during 1 week all the samples have gained about 0.6–0.75 g without any apparent trend among the different materials. If we wanted to correlate the enzymatic hydrolysis rate to hydrophilicity, as calculated from contact angles, we should expect PPSeb/MMT to have the highest enzymatic hydrolysis rate, since it is the most hydrophilic, and PPSeb/MWCNT the lowest. However, according to mass loss data, PPSeb has the highest mass loss, while PPSeb/SiO$_2$ nanocomposite with similar contact angle has the lowest. The other nanocomposites have intermediate values even though PPSeb/MMT is the most hydrophilic. In similar nanocomposites of PLLA with magnesia nanoparticles (PLLA/g-MgO) it was found that the degradation rate of the nanocomposites increases with the g-MgO nanoparticles content [40]. This result was attributed to the higher water absorption by the nanocomposites as compared with the neat polymer, which allows for faster hydrolytic degradation. However, all of our nanocomposites exhibit lower degradation rates than PPSeb. Taking all these into account it is concluded that the hydrophilicity of the sample does not play an important role in the extent of enzymatic hydrolysis.

From the above results it can be seen that the presence of nanoparticles is the main reason for the lower enzymatic hydrolysis rates of the nanocomposites as compared to neat PPSeb. This can be explained by taking into account that the first step during enzymatic hydrolysis is the surface adsorption of the enzyme. As a large portion of the outer surface of the polymer sample is replaced by the inorganic nanoparticles the total surface available for enzymatic hydrolysis is significantly reduced, leading to reduced enzymatic hydrolysis rates and mass loss. The higher degree of crystallinity and melting point of nanocomposites, as well as their lower crystallite sizes, could also have a minor influence on their lower enzymatic

Table 2
Thermal properties and degree of crystallinity of PPSeb and its nanocomposites during enzymatic hydrolysis at different hydrolysis times.

Sample	Enzymatic hydrolysis time																			
	0 h					24 h					72 h					192 h				
	T_{m1} (°C)	T_{m2} (°C)	T_c (°C)	ΔH_m (J/g)	X_c (%)	T_{m1} (°C)	T_{m2} (°C)	T_c (°C)	ΔH_m (J/g)	X_c (%)	T_{m1} (°C)	T_{m2} (°C)	T_c (°C)	ΔH_m (J/g)	X_c (%)	T_{m1} (°C)	T_{m2} (°C)	T_c (°C)	ΔH_m (J/g)	X_c (%)
PPSeb	55.3	51.2	30.2	58.9	42.1	58.2	52.2	31.6	64.4	46.1	59.7	53.7	32.3	66.9	47.8	–	–	–	–	–
PPSeb/SiO$_2$	62.1	47.5	30.8	64.8	46.3	60.9	49.3	33.4	67.9	48.5	59.8	51.2	33.8	68.6	49.0	58.1	49.1	34.4	69.3	49.5
PPSeb/MMT	60.3	47.2	29.1	64.6	45.4	59.3	50.1	30.4	67.6	48.3	58.1	51.8	31.4	68.4	48.9	58.4	52.8	31.1	67.9	48.5
PPSeb/MWCNTs	59.4	45.6	41.1	65.7	48.4	59.6	48.3	42.2	68.4	48.9	59.8	50.7	42.1	69.5	49.6	57.2	52.6	42.2	68.9	49.2
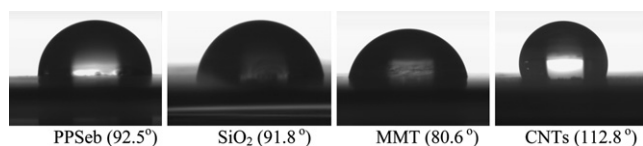
Fig. 7. Contact angles of PPSeb and its nanocomposites.

Table 3
Characteristic binding energies of carbonyl and oxygen components in PPSeb and its nanocomposites.

Component	Peak position (eV)			
	PPSeb	PPSeb/SiO$_2$	PPSeb/MMT	PPSeb/MWCNTs
C$_1$	284.54	284.65	284.60	284.60
C$_2$	285.39	285.49	285.36	285.28
C$_3$	286.63	286.84	286.66	286.68
C$_4$	289.10	289.20	289.08	289.11
O$_1$	532.21	531.78	531.96	532.24
O$_2$	533.51	533.66	533.57	533.52

Where: C$_1$ = CC and CH, C$_2$ = βC to ester, C$_3$ = C-O, C$_4$ = ester (C=O)-O, O$_1$ = ester(C=O)-O and O$_2$ = carbonyl (C=O).

hydrolysis rates compared with neat PPSeb. However, this view cannot explain why the nanocomposites, which have similar degrees of crystallinity and melting points, have different hydrolysis rates. It seems that the type of nanoparticle and the interactions that ensue between PPSeb matrix and nanoparticles upon mixing is the main reason for the different mass losses observed.

In order to confirm the interactions between PPSeb and nanoparticles XPS analysis was performed. Neat PPSeb has characteristic peaks at the regions C1s and O 1s with binding energies 283–292 eV and 529–536 eV, respectively. Both peaks can be further analyzed to different binding energies corresponding to different carbonyl components like C$_1$ = CC and CH (284.54 eV), C$_2$ = βC to ester (285.39 eV), C$_3$ = C-O (286.63 eV), C$_4$ = ester (C=O)-O (289.10 eV) and oxygen like O$_1$ = ester(C=O)-O (532.21 eV) and O$_2$ = carbonyl (C=O) (533.51 eV) (Fig. 8). All the binding energies of the studied samples are presented in Table 3. Comparing the carbonyl group binding energies between neat PPSeb and its nanocomposites it can be seen that these are almost identical in all samples. However, same small differences were recorded in the oxygen region and mainly of the O$_1$ ester group in the samples containing SiO$_2$ and MMT. These values are slightly to lower binding energies indicating the existence of some interactions between PPSeb and these nanoparticles. In the case of PPSeb/MWCNTs the binding energy of O$_1$ is at the same position as in the neat PPSeb (532.24 eV), which is a proof that MWCNTs cannot participate at any kind of interactions. This finding could explain why PPSeb/MWCNTs nanocomposite has the higher enzymatic hydrolysis rate from the other two nanocomposites.

In the case of PPSeb/MMT nanocomposite examining the binding energies of O 1s at 532.16 eV, Si 2p at 102.9 eV and Al 2p at 74.8 eV the formation of new covalent bonds should be excluded, since new peaks were not formed. Thus, it is possible that these interactions correspond to weak hydrogen bonding. Such reductions of the biodegradation rate have also been linked by others to the interactions between the matrix and the clay nano-filler [13]. This conclusion is strengthened by the small shift of the binding energy of O$_1$ (Fig. 9a). However, in the case of PPSeb/SiO$_2$ nanocomposites it was clearly the formation of covalent bonds between SiO$_2$ nanoparticles and PPSeb macromolecular chains (Fig. 9b). The peak at 101.94 eV is the binding energy of Si–O–H, which is in accordance with values reported in the literature [41]. After the peak analysis in Si 2p region of XPS spectrum of PPSeb/SiO$_2$ nanocomposite, it can be seen that a new chemical bond (Si–O–C) is formed by the reaction between Si–OH and the hydroxyl end groups of PPSeb. The binding energy of this new peak is 102.78 eV. The formation of such chemical bond was also verified by XPS spectroscopy in our previous paper in poly(propylene succinate)/SiO$_2$ nanocomposites [18] as well as in poly(L-lactide)/SiO$_2$ nanocomposites [42]. The formation of covalent bonds between SiO$_2$ nanoparticles and PPSeb macromolecules should be the main
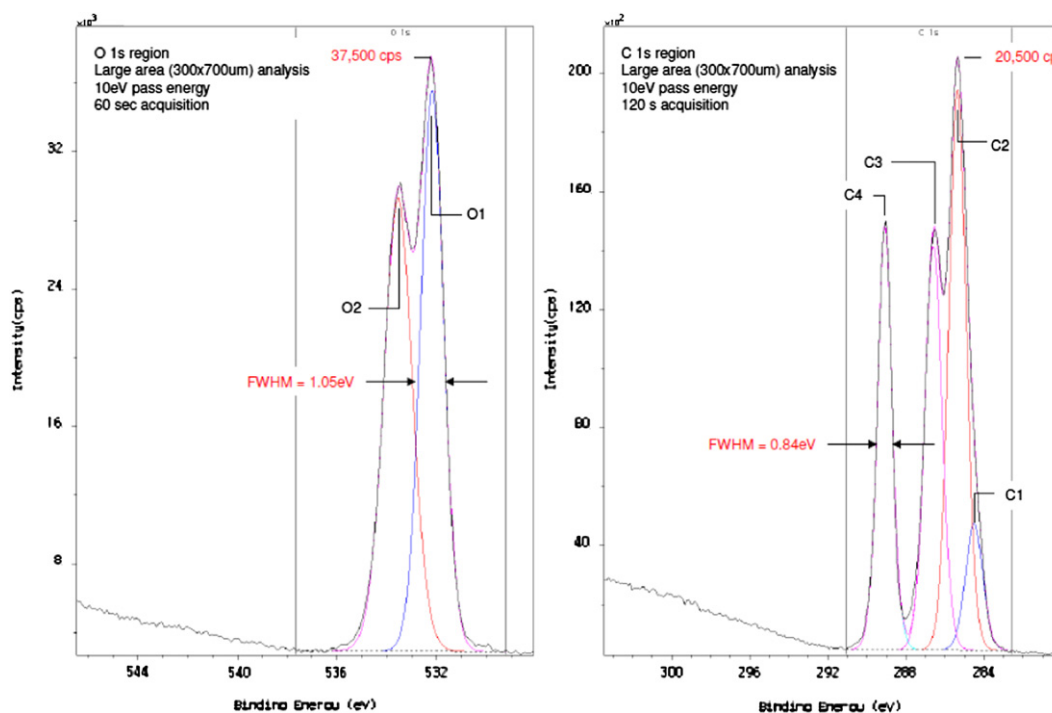

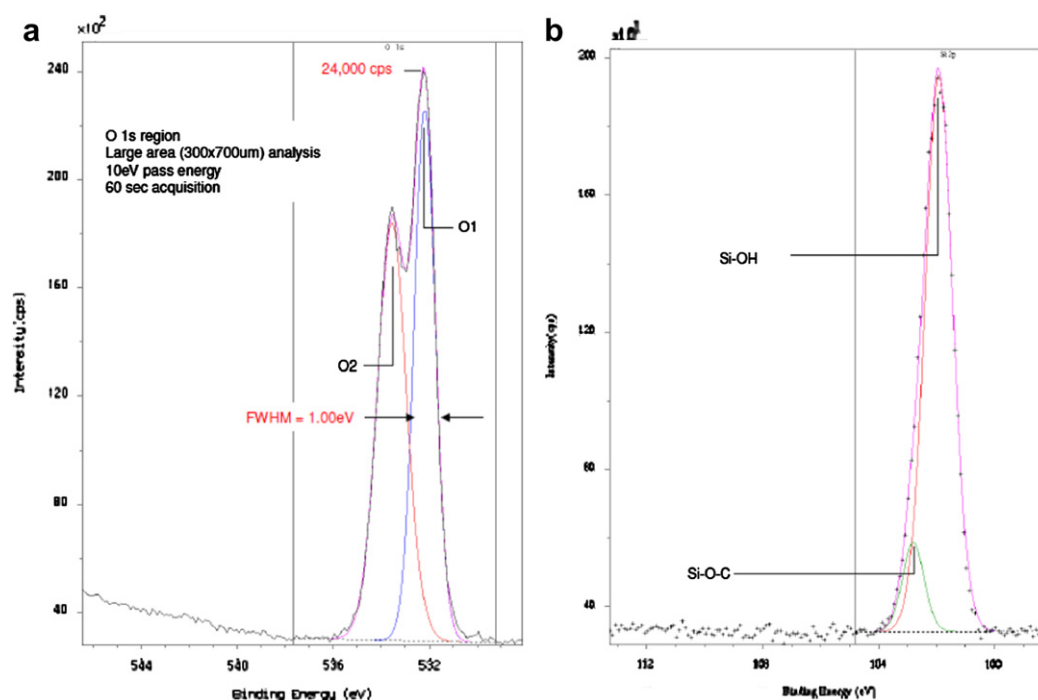Fig. 8. XPS spectra of PPSeb in O 1s and C 1s regions.

Fig. 9. XPS spectra of a) PPSeb and b) PPSeb/MMT nanocomposite in O 1s region.

reason for the low enzymatic hydrolysis rate of this particular nanocomposite.

3.3. Enzymatic hydrolysis mechanism

The hydrolysis of polyester seems to mainly proceed by an enzymatic surface mechanism involving a number of phenomena. Initially, water absorption is taking place followed by ester cleavage by hydrolysis and formation of oligomer fragments. Some of these fragments, depending on their molecular weight, are soluble and can diffuse through the bulk matrix into the liquid medium. This causes a reduction in mass loss to be observed (Fig. 4). Since this reduction is dependent on the kind of nanoparticles employed we may hypothesize for a moment that the mechanism of enzymatic hydrolysis in nanocomposites is somewhat different from that in neat PPSeb. To examine this hypothesis, in addition to mass loss measurements, the molecular weight variation and identity of the soluble fragments into the liquid medium during enzymatic hydrolysis will have to be characterized.

As can be seen from Table 4 the reduction in molecular weight of PPSeb and its nanocomposites starts from the first 24 h of hydrolysis and increases progressively. After 72 h of enzymatic hydrolysis, higher molecular weight decreases were obtained for neat PPSeb by approximately 50%, PPSeb/MWCNTs by app. 28%, PPSeb/MMT by app. 24%, and PPSeb/SiO$_2$ by app. 14% (Table 4). This, in accordance with mass loss data, indicates that PPSeb is degraded faster than its nanocomposites. The progressive increase of Mw/Mn for PPSeb and its nanocomposite with MWCNTs after the first days of hydrolysis is due to the macromolecular chain scission occurring during enzymatic hydrolysis, increasing the fraction of oligomers and lower molecular weight molecules in the bulk material. However, this increase is smaller in nanocomposites containing SiO$_2$ and MMT as a consequence of the lower enzymatic hydrolysis rate exhibited by these materials. Taking into account the progressive molecular weight reduction after 24h of enzymatic hydrolysis, it can be assumed that endo- type hydrolysis is taking place, which degrades

the length of the macromolecular chains. This is in line with our previous observations for similar polyesters [1]. However, the high mass loss, especially in neat PPSeb, is an indication that the generation of soluble fragments from macromolecular ends occurs simultaneously with macromolecular chain scission. In other words, it seems that enzymatic hydrolysis via an exo- type mechanism occurs simultaneously with the endo- type. The mechanism seems to be similar in neat PPSeb and its nanocomposites, although the molecular weight reduction is slower in nanocomposites. However, the addition of nanoparticles and more preferably SiO$_2$ reduces the polymer degradation extent which is in accordance with a previous study from Fukushima et al. [28]. In addition to fumed silica, TiO$_2$ nanoparticles were also reported to inhibit the decomposition rate of PBSu under enzymatic treatment [43]. This is because TiO$_2$ particles can inhibit the diffusion and adsorption of enzyme molecules onto the PBSu surface from an aqueous solution. Maybe a similar mechanism is taking place in our nanocomposites.

However, the molecular weight reduction seems to be lower than the mass loss reductions (Fig. 4) in all cases. This is because enzymatic hydrolysis is a phenomenon that occurs mainly at the solid/solution interface, hence the molecular weight in the bulk of the material remains almost unaffected. In a recent study involving GPC measurements made on PCL nanocomposites before and after degradation an increase in the average molecular weight was observed as a result of biodegradation [44]. Degradative processes

Table 4
Molecular weights and polydispersity (PD) variation of PPSeb and its nanocomposites during enzymatic hydrolysis ad different times (0, 24, 72 and 192 h).

Samples	Mn (g/mol)				PD (Mw/Mn)			
	0 h	24 h	72 h	192 h	0 h	24 h	72 h	192 h
PPSeb	35260	31180	17737	–	1.87	1.92	2.04	–
PPSeb/SiO$_2$	52680	45602	45223	43163	1.64	1.75	1.76	1.80
PPSeb/MMT	50790	46384	38470	35257	1.70	1.74	1.78	1.87
PPSeb/MWCNTs	46570	39040	33521	30580	1.71	1.85	1.96	2.17
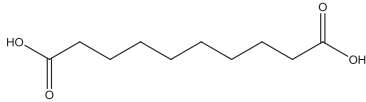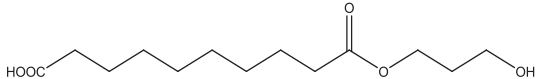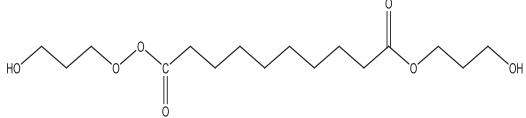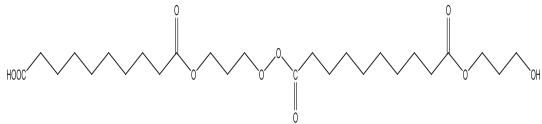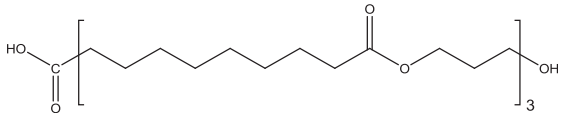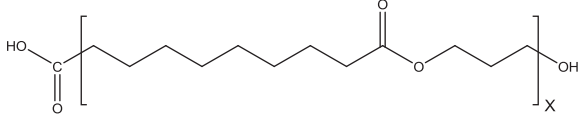
therefore preferentially attack shorter chains, those which tend to be more involved in the amorphous phase, and therefore, they subtract short chains from the system, resulting in an increase in average molecular weight.

The molecular weight reduction was also compared with the identification of the fragments that have been removed during hydrolysis and are soluble in the liquid buffer. Their ion masses are characterized with LC-MS and possible structures of these are
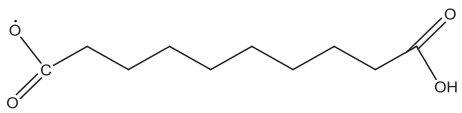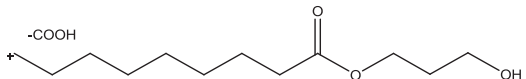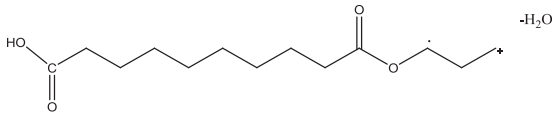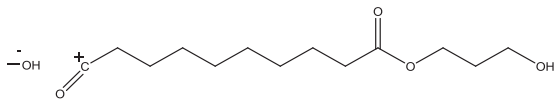
Table 5
Possible ion mass fragments removed during enzymatic hydrolysis from PPSeb and its nanocomposites (Seb: sebacic acid and PD:1,3-propylene glycol).

Molecular formula	Chemical structure	Abbreviation	m/z
Sebacic Acid		Seb	202
Monomer		PD-Seb	260
Monomer		PD-Seb-PD	318
Dimer		PD-Seb—PD-Seb	520
Trimer		(PD-Seb)$_3$	744
Oligomer		(PD-Seb)$_x$	–
Monomer end-groups		Seb (-H$^-$)	201
Monomer end-groups		PD-Seb (−COOH)	215
Monomer end-groups		PD-Seb (−H$_2$O)	241
Monomer end-groups		PD-Seb (−OH)	243
Oligomer end-groups	HO——(PDSeb)$_x$——OH	OH-(PD-Seb)$_x$-OH	–
Oligomer end-groups	HO——(PDSeb)$_x$——COOH	OH-(PD-Seb)$_x$-COOH	–
Oligomer end-groups	HOOC——(PDSeb)$_x$——COOH	HOOC-(PD-Seb)$_x$-COOH	–
Oligomer end-groups	HO——(PDSeb)$_x$——COH	HO-(PD-Seb)$_x$-COH	–

Table 6

Ion mass fragments of PPSeb and its nanocomposites during enzymatic hydrolysis at different hydrolysis times (24, 72 and 192 h) detected with LC-MS (m/z = ion mass and RI = relative intensity).

Samples		PPSeb			PPSeb/SiO$_2$			PPSeb/MWCNTs			PPSeb/MMT		
Enzymatic hydrolysis time		24h	72h	192h	24h	72h	192h	24h	72h	192h	24h	72h	192h
Fragments	m/z	RI	RI	RI	RI	RI	RI	RI	RI	RI	RI	RI	RI
HOOC-Seb-COOH	201	90	100	100	100			50			100		
PD-Seb (−OH)	243	100	90		100	70		100	70	50	100	70	50
PD-Seb	259	90		20	100				100	100	100		40
PD-Seb-PD	318				100	20						100	
Seb-PD-Seb (−H$_2$O)	426							80					
PD-Seb-PD-Seb	443	30		70	30			100	80		100		100
PD-Seb-PD-Seb (−OH)	486				30		100						
(PD-Seb)$_2$-PD (-2xH$_2$O)	525		25									80	
(PD-Seb)$_2$-PD	560		15			80			90			30	
Seb-(PD-Seb)$_2$ (−H$_2$O)	666											90	100
Seb-(PD-Seb)$_2$	686		20			70			80				100
(PD-Seb)$_3$-PD (−H$_2$O)	784		70										
(PD-Seb)$_3$-PD	802					70							
Seb-(PD-Seb)$_3$ (−OH)	911											100	90
Seb-(PD-Seb)$_3$	924											30	
Seb-(PD-Seb)$_3$-PD (−COOH)	939								40				
Seb-(PD-Seb)$_3$-PD (−H$_2$O)	965					100			100				
(PD-Seb)$_4$-PD	1044			50									60
Seb-(PD-Seb)$_4$ (-2xCOOH)	1080			100						100			
Seb-(PD-Seb)$_4$	1170									100			90
(PD-Seb)$_5$	1222			100									
(PD-Seb)$_5$-PD	1286									100			100
Seb-(PD-Seb)$_5$ (−OH)	1350												30
Seb-(PD-Seb)$_5$	1367									70			
(PD-Seb)$_6$ (−COOH)	1425						100						
(PD-Seb)$_6$	1453						50						
(PD-Seb)$_6$-PD (−H$_2$O)	1510						100						
Seb-(PD-Seb)$_6$	1654												
(PD-Seb)$_6$-PD	1770						100						
Seb-(PD-Seb)$_7$-PD	1952						20						

presented in Table 5. These are monomers such as sebacic acid, 1,3-propylene glycol with sebacic acid, dimmers and trimers between propanediol and sebacic acid as well as oligomers with molecular weights till 2000 g/mol. 1,3-propanediol could not be detected since it was not possible to detect ion fragments with molecular weights smaller that 100 g/mol. The exact molecular form of each fragment at different enzymatic hydrolysis times for each one of the materials studied is presented in Table 6.

As can be seen in Table 6 fragments with molar masses less than 443 are formed in all samples after 24 h of enzymatic hydrolysis. These fragments are attributed to sebacic acid, monomers between sebacic acid and 1,3-propanediol and dimmers like PD-Seb-PD-Seb. In such a case macromolecules degrade from their ends and as a result water-soluble oligomers are formed and then removed from the film surface. Such water-soluble monomers and co-oligomers produced by hydrolysis were extensively studied in hydrolysis of poly(butylene succinate-co-butylene sebacate)s, P(BS-co-BSe) and poly(butylenes succinate-co-butylene adipate)s, P(BS-co-BA) by using *Mucor miehei* and *R. arrhizus* [45]. For this reason the weight of films was decreased during enzymatic hydrolysis due to oligomers' removal. After 72 h of enzymatic hydrolysis, in addition to the by-products mentioned above, some fragments with higher molar masses such as, (PD-Seb)$_2$-PD, Seb-(PD-Seb)$_2$(-H$_2$O), Seb-(PD-Seb)$_2$, etc., are also identified in all samples. Differences between the soluble fragments in the samples studied cannot be identified during the first 92 h of hydrolysis, which does not allow us to assess the effect of nanoparticle type on the enzymatic hydrolysis mechanism of PPSeb during this time. Differences are detected after 192 h of enzymatic hydrolysis. In all samples sebacic acid, and monomers between sebacic acid and 1,3-propanediol such as PD-Seb-PD-Seb are identified. However, fragments with higher

ion masses such as (PD-Seb)$_4$-PD, Seb-(PD-Seb)$_4$ (-2xCOOH) and Seb-(PD-Seb)$_4$ also are identified for the first time in PPSeb and nanocomposites with MWCNTs and MMT. In the case of PPSeb/SiO$_2$ nanocomposite such fragments were not detected but only fragments with higher ion masses (1425−1952) like (PD-Seb)$_6$ (-COOH), (PD-Seb)$_6$, (PD-Seb)$_6$-PD (-H$_2$O), Seb-(PD-Seb)$_6$, (PD-Seb)$_6$-PD were found. This is clear evidence that, in the case of nanosilica, the hydrolysis from the macromolecular ends becomes more difficult as the enzymatic hydrolysis proceeds. This could be attributed to the covalent interactions between silica nanoparticle surface groups - PPSeb macromolecular ends, which sterically inhibit enzymatic hydrolysis.

4. Conclusions

PPSeb nanocomposites containing 2 wt% SiO$_2$, MWCNTs or MMT were found to exhibit improved mechanical properties compared with neat PPSeb due to the reinforcement effect cause by the presence of nanoparticles. Thermal properties such as melting point and degree of crystallinity of PPSeb were also higher in nanocomposites since nanoparticles can act as nucleating agents increasing the degree of crystallinity.

In terms of enzymatic hydrolysis, lower rates of mass loss were observed for the nanocomposites. Since the procedure of enzymatic hydrolysis is directly dependent on the available surface area of the sample, and considering that the nanoparticles employed here cannot be degraded by lipases, their addition causes an overall reduction of available surface area for hydrolysis. Enzymatic hydrolysis is taking place primary in the amorphous domain of the polymer matrix. The nanocomposites exhibited thicker lamellae and more crystalline stacks, and therefore, they degrade slowly and to a lesser extent than neat PPSeb. Therefore, the higher degree of crystallinity

observed in nanocomposites could also have a small effect on the reduced enzymatic hydrolysis rates.

Another possible cause of the observed behaviour is the interactions between nanoparticles and PPSeb. SiO$_2$ nanoparticles can form covalent bonds with PPSeb macromolecules and thus exhibit the lowest enzymatic hydrolysis rates compared to the other nanocomposites. For this reason the absence of any kind of interactions between MWCNTs and PPSeb leads to higher enzymatic hydrolysis rate, while MMT seems to form week interactions with PPSeb and thus has intermediate rates.

With respect to the mechanism of enzymatic hydrolysis, this was found from LC-MS to be similar in neat PPSeb and its nanocomposites.

Acknowledgement

References

[1] Bikiaris DN, Papageorgiou GZ, Achilias DS. Synthesis and comparative biodegradability studies of three poly(alkylene succinate)s. Polym Degrad Stab 2006;91:31–43.

[2] Bikiaris DN, Papageorgiou GZ, Giliopoulos DJ, Stergiou CA. Correlation between chemical and solid-state structures and enzymatic hydrolysis in novel biodegradable polyesters. The case of Poly(propylene alkanedicarboxylate)s. Macromol Biosci 2008;8:728–40.

[3] Yang KK, Wang XL, Wang YZ. Progress in nanocomposite of biodegradable polymer. J Ind Eng Chem 2007;13:485–500.

[4] Zhou Q, Xanthos M. Nanoclay and crystallinity effects on the hydrolytic degradation of polylactides. Polym Degrad Stab 2008;93:1450–9.

[5] Arena M, Abbate C, Fukushima K, Gennari M. Degradation of poly (lactic acid) and nanocomposites by Bacillus licheniformis. Environ Sci Pollut Res doi:10.1007/s11356-011-0443-2.

[6] Li Q, Yoon JS, Chen GX. Thermal and biodegradable properties of poly(L-lactide)/poly(ε-Caprolactone) compounded with functionalized organoclay. J Polym Environ 2011;19:59–68.

[7] Lee SR, Park HM, Lim H, Kang T, Li X, Cho WJ, et al. Microstructure, tensile properties, and biodegradability of aliphatic polyester/clay nanocomposites. Polymer 2002;43:2495–500.

[8] Ray SS, Yamada K, Okamoto M, Ueda K. Control of biodegradability of polylactide via nanocomposite technology. Macromol Mater Eng 2003;288:203–8.

[9] Singh NK, Purkayastha BD, Roy JK, Banik RM, Yashpal M, Singh G, et al. Nanoparticle-induced controlled biodegradation and its mechanism in poly(ε-caprolactone). ACS Appl Mater Interf 2010;2:69–81.

[10] Han SI, Lim JS, Kim DK, Kim MN, Im SS. *In situ* polymerized poly(butylene succinate)/silica nanocomposites: physical properties and biodegradation. Polym Degrad Stab 2008;93:889–95.

[11] Chouzouri G, Xanthos M. Degradation of aliphatic polyesters in the presence of inorganic fillers. J Plast Film Sheet 2007;23:19–36.

[12] Chouzouri G, Xanthos M. In vitro bioactivity and degradation of polycaprolactone composites containing silicate fillers. Acta Biomater 2007;3:745–56.

[13] Maiti P, Batt CA, Giannelis EP. New biodegradable polyhydroxybutyrate/layered silicate nanocomposites. Biomacromolecules 2007;8:3393–400.

[14] Fukushima K, Tabuani D, Abbate C, Arena M, Ferreri L. Effect of sepiolite on the biodegradation of poly(lactic acid) and polycaprolactone. Polym Degrad Stab 2010;95:2049–56.

[15] Fukushima K, Abbate C, Tabuani D, Gennari M, Rizzarelli P, Camino G. Biodegradation trend of poly(ε-caprolactone) and nanocomposites. Mater Sci Eng C 2010;30:566–74.

[16] Manoudis PN, Karapanagiotis I, Tsakalof A, Zuburtikudis I, Panayiotou C. Superhydrophobic composite films produced on various substrates. Langmuir 2008;24:11225–32.

[17] Vassiliou A, Bikiaris D, El Mabrouk K, Kontopoulou M. Effect of evolved interactions in poly(butylene succinate)/fumed silica biodegradable in situ prepared nanocomposites on molecular weight, material properties, and biodegradability. J Appl Polym Sci 2011;119:2010–24.

[18] Kostoglou M, Bikiaris D. Kinetic analysis of nanocomposites prepared in situ consisting of an aliphatic biodegradable polyester and fumed silica nanoparticles. Macromol React Eng 2011;5:178–89.

[19] Vassiliou AA, Papageorgiou GZ, Achilias DS, Bikiaris DN. Non-isothermal crystallisation kinetics of in situ prepared poly(ε-caprolactone)/surface-treated SiO$_2$ nanocomposites. Macromol Chem Phys 2007;208:364–76.

[20] Bikiaris D, Karavelidis V, Karayannidis GA. New approach to prepare poly(ethylene terephthalate)/silica nanocomposites with increased molecular weight and fully adjustable branching or crosslinking by SSP. Macromol Rapid Comm 2006;27:1199–205.

[21] Wang F, Meng X, Xu X, Wen B, Qian Z, Gao X, et al. Inhibited trans-esterification of PET/PBT blends filled with silica nanoparticles during melt processing. Polym Degrad Stab 2008;93:1397–404.

[22] Yao X, Tian X, Xie D, Zhang X, Zheng K, Xu J, et al. Interface structure of poly(ethylene terephthalate)/silica nanocomposites. Polymer 2009;50:1251–6.

[23] Bikiaris DN, Vassiliou AA. Nanocomposite coatings and nanocomposite materials [Chapter 4]. In: Öchsner A, Ahmed W, Ali N, editors. Fumed silica reinforced plastics. Switzerland: Trans Tech Publications Ltd; 2009.

[24] Bikiaris D, Prinos J, Botev M, Betchev C, Panayiotou C. Blends of polymers with similar glass transition temperatures: a DMTA and DSC study. J Appl Polym Sci 2004;93:726–35.

[25] Vladimirov V, Betchev C, Vassiliou A, Papageorgiou G, Bikiaris D. Dynamic mechanical and morphological studies of isotactic polypropylene/fumed silica nanocomposites with enhanced gas barrier properties. Comp Sci Technol 2006;66:2935–44.

[26] Kontou E, Niaounakis M. Thermo-mechanical properties of LLDPE/SiO$_2$ nanocomposites. Polymer 2006;47:1267–80.

[27] Bordes P, Pollet E, Avérous L. Nano-biocomposites: biodegradable polyester/nanoclay systems. Prog Polym Sci 2009;34:125–55.

[28] Fukushima K, Tabuani D, Abbate C, Arena M, Rizzarelli P. Preparation, characterization and biodegradation of biopolymer nanocomposites based on fumed silica. Eur Polym J 2011;47:139–52.

[29] Wu K, Wu C, Chang J. Biodegradability and mechanical properties of poly-caprolactone composites encapsulating phosphate-solubilizing bacterium *Bacillus* sp. PG01. Process Biochem 2007;42:669–75.

[30] Lee SK, Seong DG, Youn JR. Degradation and rheological properties of biodegradable nanocomposites prepared by melt intercalation method. Fibers Polym 2005;6:289–97.

[31] Qiu Z, Ikehara T, Nishi T. Poly(hydroxybutyrate)/poly(butylene succinate) blends: Miscibility and nonisothermal crystallization. Polymer 2003;44:2503–8.

[32] Gan Z, Abe H, Kurokawa H, Doi Y. Solid-state microstructures, thermal properties, and crystallization of biodegradable poly(butylene succinate) (PBS) and its copolyesters. Biomacromolecules 2001;2:605–13.

[33] Marten E, Müller RJ, Deckwer WD. Studies on the enzymatic hydrolysis of polyesters - I. Low molecular mass model esters and aliphatic polyesters. Polym Degrad Stab 2003;80:485–501.

[34] Abou-Zeid DM, Müller RJ, Deckwer WD. Biodegradation of aliphatic homopolyesters and aliphatic-aromatic copolyesters by anaerobic microorganisms. Biomacromolecules 2004;5:1687–97.

[35] Tsuji H, Tezuka Y. Alkaline and enzymatic degradation of L-lactide copolymers, 1: amorphous-made films of L-lactide copolymers with D-lactide, glycolide, and ε-caprolactone. Macromol Biosci 2005;5:135–48.

[36] Papageorgiou GZ, Achilias DS, Nanaki S, Beslikas T, Bikiaris D. PLA nanocomposites: effect of filler type on non-isothermal crystallization. Thermochim Acta 2010;511:129–39.

[37] Antoniadis G, Paraskevopoulos KM, Vassiliou AA, Papageorgiou GZ, Bikiaris D, Chrissafis K. Nonisothermal melt-crystallization kinetics for in situ prepared poly(ethylene terephthalate)/monmorilonite (PET/OMMT). Thermochim Acta 2011;521:161–9.

[38] Ozkoc G, Kemaloglu S. Morphology, biodegradability, mechanical, and thermal properties of nanocomposite films based on PLA and plasticized PLA. J Appl Polym Sci 2009;114:2481–7.

[39] Papageorgiou GZ, Achilias DS, Bikiaris DN. Crystallization kinetics and melting behaviour of the novel biodegradable polyesters poly(propylene azelate) and poly(propylene sebacate). Macromol Chem Phys 2009;210:90–7.

[40] Ma F, Lu X, Wang Z, Sun Z, Zhang F, Zheng Y. Nanocomposites of poly(L-lactide) and surface modified magnesia nanoparticles: Fabrication, mechanical property and biodegradability. J Phys Chem Solids 2011;72:111–6.

[41] Li H, Wang R, Hu H, Liu W. Surface modification of self-healing poly(urea-formaldehyde) microcapsules using silane-coupling agent. Appl Surf Sci 2008;255:1894–900.

[42] Prébé A, Alcouffe P, Cassagnau Ph, Gérard JF. *In situ* polymerization of l-Lactide in the presence of fumed silica. Mater Chem Phys 2010;124:399–405.

[43] Miyauchi M, Li Y, Shimizu H. Enhanced degradation in nanocomposites of TiO$_2$ and biodegradable polymer. Environ Sci Technol 2008;42:4551–4.

[44] Neppalli R, Causin V, Marega C, Saini R, Mba M, Marigo A. Structure, morphology, and biodegradability of poly(e-caprolactone)-based nanocomposites. Polym Eng Sci 2011;51:1489–96.

[45] Rizzarelli P, Impallomeni G, Montaudo G. Evidence for selective hydrolysis of aliphatic copolyesters induced by lipase catalysis. Biomacromolecules 2004;5:433–44.